THE COMPARISON OF DYNAMIC EFFECTS ACTING IN THE COMMON CROSSING AND SWITCH UNIT OF A TURNOUT

Jaroslav Smutný, Dušan Janoštík*, Viktor Nohál

Institute of Railway Structures and Constructions, Faculty of Civil Engineering, Brno University of Technology, Brno, Czech republic

*E-mail of corresponding author: janostik.d@fce.vutbr.cz

Resume

The paper presents an analysis and comparison of selected dynamic parameters in the common crossing and switch unit of a railway turnout. The paper includes a description of the measurement methodology, the report of mathematical methods used to evaluate the measured data and comparison of selected parameters describing dynamic processes in individual parts of the structure. The paper also includes a mathematical analysis of the lesser-known Hilbert Huang transformation, including its practical application. From the presented case study, practical experience and recommendations for the railway line managers, research organizations and possibly for the wider technical public are derived.

Article info

Received 16 September 2021
Accepted 10 January 2022
Online 29 March 2022

Keywords:

railway turnout
common crossing unit
switch unit
dynamic effects
nonstationary and nonlinear signals
vibrations analysis in time and frequency domain
Hilbert-Huang transformation

Available online: https://doi.org/10.26552/com.C.2022.3.D116-D125

ISSN 1335-4205 (print version)
ISSN 2585-7878 (online version)

1 Introduction

All the parts of the superstructure and substructure are subject to dynamic loads from the running of trains. When the train is moving, the wheels of the train set not only roll on the rail but also shift tangentially. In addition, slip occurs at small radii of curves. The forces and moments are then not transmitted pointwise, but in the contact area between the wheel and the rail.

The axle forces acting vertically on the rail, derived by the own weight of the trainset, the longitudinal stresses caused by starting and braking, the longitudinal and transverse pressures and the forces generated by passing in a curve, etc., are distributed through the rail fastening to the rail supports, the track bed and the subgrade. The whole process of dynamic loading is accompanied by the propagation of vibrations, changes in motion behavior or deformation of the structure [1].

When passing the axle wheels on rails, it is necessary to consider the uneven distribution of stress in individual and adjacent areas of supports and rail bed. The rails distribute the load caused by the running trainsets to individual sleepers. The magnitude of the forces that the rail transmits on the sleeper is determined by the shape of the rail, the flexibility of the rail mounting on the sleeper, the shape of the sleeper and the distribution of the sleepers. The rail bed is then stressed unevenly depending on how the stress is distributed over the sleeper bed [2]. This is also related to the uneven stress on the bottom of the railway.

The transmission of dynamic forces from the rails to the subsoil is even more complicated in turnout constructions. It is necessary to include the changing position of the rails in the transverse direction on the supports, uneven transmission of dynamic effects in different parts of the turnout structure, changing cross-sections of rails in the tongue, crossing the wheelsets retainer, or the changing longitudinal dimension of the rail supports.

The dynamic effects on the railway structure increase with increasing speed of the trainsets. The dynamic stress of the track is also influenced by properties of all the parts of the railway superstructure, i.e. the quality of the gravel bed, the type of sleepers, the quality of their tamping, the properties of track fittings, the type of fasteners and the quality of the railway sub-ballast layers, as well. Particularly at points of interruption in the continuity of travel and at points of change in track stiffness, there are increased dynamic effects. In those places, there is an irregular settlement of the rail bed,

crushing of the aggregate of the rail bed and defects on the running surface of the rails.

One of the main problems of today's railways is to minimize the costs associated with track maintenance. Based on the knowledge of the dynamic processes taking place in it, it is possible to determine appropriate measures that will lead to minimization of the maintenance costs. Effective tools also include vibrodiagnostics, i.e. the analysis of vibrations propagating through the superstructure and substructure. Therefore, one will increasingly encounter phenomena whose satisfactory clarification and technical solution will depend on understanding the dynamic stress of the railway structure [3].

The railway turnout structures represent one of the key points of the railway transport. This is because a turnout structure consists of a number of structural components of different properties, which in summary must fulfil the required functions. Among the most important properties is especially their reliability and safety within the framework of the railway operation. At the same time, the running of trainsets generates large dynamic stress in the turnout area, which is different from the dynamic stress in the rail grid area. Therefore, it is very important to study the dynamic processes in turnouts in order to improve the quality of maintenance work. Application of the new methods of measurement and analysis helps to achieve that goal [4].

A classic simple turnout consists of three main parts - common crossing unit, closure unit and switch unit (Figure 1). The common unit consists of a frog, a retainer and an outer rail. There is a crossing of rails and separation of rails in two different directions. The common crossing unit forms the place where the wheel passes a gap (depression) for the wheel flange of the vehicle, which moves in another direction. In order to avoid an impact or climbing of the flange on the tip of the common crossing unit, the second wheel of the same wheelset is guided by a retaining device, which does not allow it to move away from the outer rail.

The closure unit of the turnout actually forms a tangle of tracks. It connects the switch and the common crossing unit. The interchange is a moving part of the turnout, on which the track branches in two directions. The main parts of the switch unit consist of tongues, supports and a turnout. The tongue forms the only moving structure of the carriageway. The position of the tongues determines the direction of further movement of the train set while driving. The tongues are usually stored on stool bases. Under the normal circumstances, one tongue always rests on the support. A motorized converter is used to adjust the tongues. To secure them in the appropriate position there is a locking device. From the above, it is clear that especially the common crossing and switch units belong to the key parts of turnouts in terms of dynamic effects.

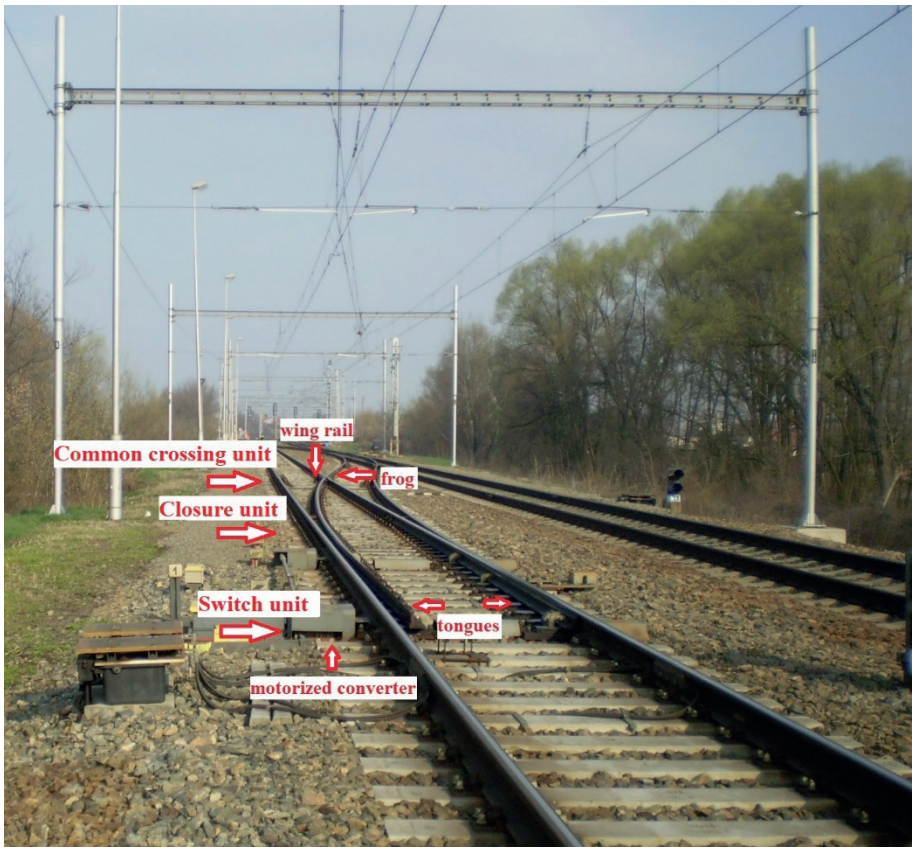

Figure 1 *The picture of a turnout with a description of the most important parts*

(a) *(b)*

Figure 2 *The view of the common crossing (a) and a switch (b) unit of turnout*

The dynamic processes in both areas are further briefly considered.

High dynamic forces and high vibrations level can be expected in the area of the train set wheel transition from the wing rail to the tip of the frog, where, depending on the quality of the transition geometry, a dynamic impact occurs.

From theoretical assumptions and computer simulations [5], it is concluded that another area requiring increased attention is the switch unit. The mechanism of vibrations transmission in this case is different from that of the common crossing assembly. At the same time, many theoretical works show a lower level of vibrations propagating through the switch unit into the gravel bed. This is due to the uninterrupted running surface of the rail when the wheel flange gradually approaches and rests on the tongue rail. The intensity of vibrations is damped by the track skeleton, when a small part is damped already in the rail and its rubber pad. Further vibrations damping occurs in the sleeper. The undamped component of the vibrations energy is also transferred to the gravel bed. The question is how much of this energy is compared to the energy propagating in the common crossing unit.

2 Methods of measurement and evaluation

A measurement methodology, certified by the Ministry of Transport of Czech Republic, was used to measure the dynamic effects acting on the turnout [6]. This methodology consists of three parts. The first involves measuring the motion behavior of a structure. The second area involves the propagation of vibrations and shocks from the wheel-rail contact, through the sleeper, into the gravel bed of the common crossing and switch unit. The third area provides information on the forces and deformations acting. Note that a simplified variant of this methodology was used in this paper to present the results.

Before measuring the dynamic characteristics of the turnout, the geometric parameters were measured by a measuring wagon of the infrastructure manager in the Czech Republic. The measurement confirmed that the whole turnout is in excellent condition.

In total, two basic measuring areas with 3 measuring points were set in the measured turnout, to which piezoelectric acceleration sensors from the Bruel&Kjaer company were attached. These locations were chosen so that the measured values could be compared. In the case of the common crossing unit, it was a triaxial acceleration sensor located at the foot of the wing rail in the straight branch of the turnout (labelling outputs A4Z, A5X, A6Y), acceleration sensor located on the sleeper near the tip of the common crossing unit (A3Z) and acceleration sensor located on the rod (waveguide) in a gravel bed (A0Z). In the switch unit, the sensors were placed on the heel of the support (acceleration sensor, labelling A4Z, A5X, A6Y), then on the sleeper in the area of the passage of the wheel from the support to the tongue rail (A3Z) and measuring rod, which was embedded in the gravel bed near the passage of the wheel (A0Z). Simultaneously with the measurement of vibrations characteristics, a large number of other parameters were measured. Their comparison and analysis are not part of this paper.

Time, frequency and time-frequency analysis were used for vibrations analysis. Note that the analysis in the time plane was focused on the one hand to determine the maximum values of vibrations acceleration and on the other hand to calculate the effective value of vibrations acceleration. Within the frequency analysis, the classical Fourier analysis with output to amplitude frequency spectra was used. The formulas and the procedure for calculating the effective value of acceleration or amplitude spectra are not given in the paper, they can be found in many professional publications [7-8].

In the time-frequency analysis, the authors used the Hilbert Huang transform. According to the research and the authors' experience, this type of analysis is particularly advantageous in the case of impact loads. Since this is a less known transformation procedure with specific calculation, its analysis and description are

given in the text below.

The Hilbert-Huang transformation is a lesser-known and less widely used method for analysis of the transient, nonlinear and non-stationary signals [9-11]. The procedure for calculating this transformation must be divided into two parts. In the first part, the so-called empirical modal decomposition is performed, followed by the second in the framework, which calculates the so-called Hilbert spectrum. This then represents the propagation of energy in the time-frequency domain and is calculated by applying the well-known Hilbert transformation.

Empirical modal decomposition is used to decompose any nonlinear or nonstationary signal $s(t)$ into a finite number of eigenmodal functions. The Eigen modal functions must satisfy two basic conditions [11-12]:

- The number of extrema (i.e. minima and maxima) must be either equal to, or differ by at most one, the number of passes through the function through zero;
- At any point, the average value defined by the envelope of local maxima and local minima is zero.

The first condition is similar to the narrowband requirement for a stationary Gaussian process, the values must not differ too much. The second condition is local, derived from the first and it ensures that the instantaneous frequency will not have unnecessary fluctuations caused by the asymmetric waveforms. Note that this is essentially a resemblance to the Fourier transformation, which also decomposes into simpler functions, sins and cosines. The disadvantage of the Fourier transformation is that it gives good results only for a signal that is stationary and fully periodic. In the case of calculating the Hilbert-Huang transformation, this limit does not apply. Furthermore, the calculation procedure of the empirical modal decomposition, according to the author of the method of scientist E. Huang, is described [13-14]. The calculation procedure takes place in several steps.

The first step is to find the local extrema (maxima and minima) in the given signal $s(t)$. These extrema are then interpolated with a suitable curve, such as a cubic spline. This creates two envelopes of the original signal - the upper $e_{max}(t)$ and the lower $e_{min}(t)$. The average value of both envelopes is then calculated. Next, one calculates the difference between the signal and the mean value.

$$h_1(t) = s(t) - \mu_1(t). \tag{1}$$

If the calculation does not meet the requirements for the modal function, iterations must be continued. Note that due to the approximation, new extrema can arise, i.e. overshoot or undershoot in the envelope. The calculation procedure must be repeated until the resulting component meets the specified conditions. The procedure can be written by an equation

$$h_{k+1}(t) = h_k(t) - \mu_{k+1}(t). \tag{2}$$

It should be noted here that the iteration process essentially filters the low frequency components and smoothes the different amplitudes. The standard deviation value, which is calculated from the two consecutive results of the iteration process, was used as a criterion for completing the partial calculation of each component for the purposes of this paper. E. Huang determined a typical value of the standard deviation for the end of the iteration in the interval 0.2 and 0.3 [13-14]. Note that the first modal component represents the highest frequency component of the signal $s(t)$. If one separates the calculated component from the signal, we obtain the so-called residue. The residue contains components with lower frequencies. It can be marked as a new signal and the procedure repeated. The original signal is described by the following equation [15].

$$s(t) = \sum_{i=1}^{n} c_i + r_n, \tag{3}$$

where $s(t)$ is the original signal, r_n is the residue and c_i is the component. Equation (3) shows that the original signal can be reconstructed by simply summing all the modal functions and the residual. Note that the decomposition can be terminated based on a predetermined limit of the number of iterations or when the residual is a monotonic function from which it is no longer possible to separate other proper modal functions [16]. If one has calculated the individual components described above by decomposition, the Hilbert transformation can be applied to each and calculate the instantaneous frequency. This procedure can be expressed by the following equation.

$$s(t) = \sum_{k=1}^{n} a_k(t) \cdot e^{j \cdot \int \omega_k(t) \cdot dt}. \tag{4}$$

Thus, Equation (3) expresses the instantaneous amplitude $a_k(t)$ and the instantaneous frequency (angular frequency) $\omega(t)$ as a function of time t, while allowing the amplitude to be expressed as a function of frequency and time. It is therefore the Hilbert amplitude spectrum, which expresses the energy distribution in the time-frequency plane [17-18].

It follows from the above description that the Hilbert-Huang transformation represents an alternative to, for example, the Fourier transformation or the Wavelet transformation [19], or to other time-frequency methods, with the difference that it decomposes the measured signal in a different way. Thus, not into predefined functions such as trigonometric functions, parent wavelet etc. but into functions based on the signal under investigation.

3 The case studies

To compare the dynamic effects in the switch and the common crossing units, turnout No. 59 (Figure 2) was selected in the so-called Pardubice head of

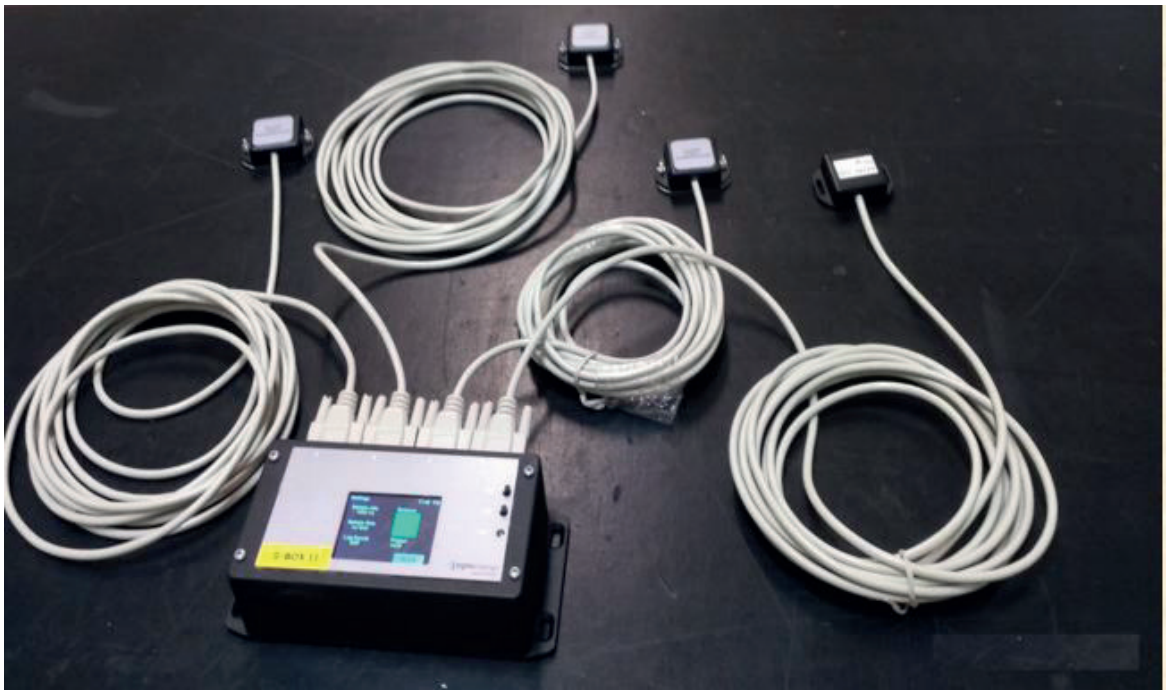

Figure 3 *View of the measuring system with sensors*

the Chocen railway station with a left turn direction (turnout designed for a speed of 80 km·h^{-1}). The selected turnout is of the type J60-1:14-760-zlp, L, p, CZP, b, KS, ZPT. Trainsets may pass through this turnout in a straight line at a line speed of 160 km·h^{-1}. The turnout is equipped with a system of railway superstructure UIC 60 with Vossloh Skl 24 fastening and concrete sleepers. Note that this is the most common type of turnout used on the corridor lines of the Czech Republic. For this reason, the author's team in this paper focused on the measurement and analysis of this particular structure. At the same time, the same types of turnouts were measured at other localities. In total, there were 20 measuring campaigns.

Two autonomous S-Box dataloggers (Figure 3), developed at the authors' workplace, were used for the measurements. The S-Box datalogger has been described in detail in the literature [20]. For measurement purposes, the measuring system was verified using a calibration sensor 8305 from Bruel&Kjaer and a vibrating calibrator V21D from Metra Mess und Frequenz Technik. It is a two-level measuring system consisting of a data logger and a superordinate computer with software for analysis of the measured data. The system provides up to 12-channel recording from various types of sensors (vibrations, noise, displacement, strain gauges, temperature etc.). Within the first level, the data is measured and stored on an SD card. The datalogger is equipped with a system to automatically start and stop recording and also provides the possibility of data wireless transmission to a higher-level system consisting of a computer and the relevant software.

Within the superordinate system (second level), manual, semi-automatic or fully automatic analysis of the measured data takes place according to a set scenario. It should be noted that for this measurement, a Raspberry Pi computer was used as the master system. The data analysis program was developed in Python. The whole setup was powered by a battery, which was recharged from a solar panel when needed. Measured and evaluated data were continuously sent to the NAS storage of the authors' workplace to the database server.

The measuring set-up was supplemented with a trigger module. This consisted of the two infrared gates mounted on a small tripod at a height of 150 mm above the top of the rail and an evaluation module. The first barrier was placed at 30 m in front of the measuring station, the second at 30 m behind it. The principle of starting and ending the measurement was based on the principle of counting and comparing the passing axles. The evaluation module simultaneously measured the running speed of the train set. This data was also transferred to the master computer.

The data filtering and classification of the trainsets into predefined categories was performed automatically on the master computer after downloading the data from the measuring system.

The evaluation software in the master computer includes implementation of the support vector machine method for recognizing the train sets. The authors of the paper have very good implementation experience with this method. The input to the method is the measured vibrations acceleration values from three sensors - on the wing rail, on the sleeper and in the gravel bed.

It should be noted that the classification software contains a database of locomotives, passenger cars and entire train sets including the gauge for more accurate recognition. The classifier was set up before the measurement.

As a part of the measurement campaign, the passage

Table 1 *The comparison of the effective values of vibrations acceleration [m.s^{-2}]*

Train set	Turnout	A0Z ^	A3Z ^	A4Z ^	A5X †	A6Y ‡	Travel speed [km/h]
Leo Express	59, Common crossing unit	20	43	108	25	32	155
	59, Switch unit	2	38	40	10	17	155
Pendolino	59, Common crossing unit	22	45	110	28	30	163
	59, Switch unit	4	39	42	12	13	162
RegioJet	59, Common crossing unit	10	26	95	17	26	140
	59, Switch unit	3	24	49	11	20	140
Train set with 151 engine	59, Common crossing unit	7	16	46	12	13	120
	59, Switch unit	2	25	42	10	14	120
Train set with 150 engine	59, Common crossing unit	2	10	33	6	10	82
	59, Switch unit	2	40	65	15	25	82

Legend: ^ in the vertical direction
† in the longitudinal direction
‡ in the transverse direction

of a total of 60 trains was recorded, for which, in addition to the time course of vibrations acceleration, their other parameters were also recorded - travel time, running speed, number of railway cars and type of locomotive and direction of travel.

For their own evaluation, these trains were divided into suitable categories. In the article, the authors focused on evaluation of selected train sets. Those were divided into three main categories. The first category includes EC trainsets. This category includes both light complete trains sets of the Pendolino and LeoExpress type, as well as classic RegioJet train sets with the E630 series locomotive. The second category is represented by the passenger trains with a locomotive of the 151 series. The third category is represented by the freight train sets hauled by relatively old locomotives of the 150 series.

The global maxima and minima were automatically subtracted in the superordinate computer, then the basic vibrations characteristics (effective acceleration values a_{ef} and amplitude frequency spectra) were calculated for each acceleration sensor and for each category of trainsets. The calculated characteristics were organized in a table and graphs for comparison. Note that the effective acceleration values shown in Table 1 are the result of averaging the partial values from all the measurements made for a given category of train set.

It is clear from Table 1 that significantly higher effective acceleration values were obtained when the EC category trainsets (Pendolino, LeoExpress and RegioJet) passed in the common crossing unit of the turnouts compared to the switch unit. Relatively similar dynamic effects were also found for passenger trains hauled by 151 series locomotives. For the trainsets hauled by Class 150 series locomotives this is different. In most of the measured parameters, higher values were obtained in the area of the exchange of the measured turnout compared to the frog part. It should be noted that this fact was also demonstrated by a more detailed analysis in the time and frequency plane, including the comparison of time records and their amplitude frequency spectra.

To compare the dynamic load found in the frog and switch unit of the turnout, the passage of a RegioJet train set at a speed of 140 kmh^{-1} was selected for the paper (Figures 4 and 5). Due to the limited space of the paper, the authors focused on a more detailed analysis of measured data from sensors that were in the gravel bed near the rail attachment. It should be noted that the RegioJet train consists of railcars from the Austrian and Swiss Federal Railways. The wagons are hauled by modernized Škoda locomotives and TRAXX MS 2e locomotives from the manufacturer Bombardier.

The top graph of each figure shows the time course of vibrations. The left graph shows the amplitude spectrum of the vibrational response. The middle graph shows the 3D representation of the time-frequency waveform of the vibrations amplitude spectrum.

The values of the spectra are expressed in decibel scale by different colours (or grayscale). Note that the maximum value is the colour black. Again, it should be mentioned that for a more detailed insight into the dynamic characteristics, time and frequency slices can be displayed within the middle graph. In the former case, those are the plots providing individual frequency spectra at different times, while in the latter case; they are the time histories of selected frequency components.

From the comparison of time records it is clear that higher values of vibrations acceleration (up to 360 m·s^{-1})

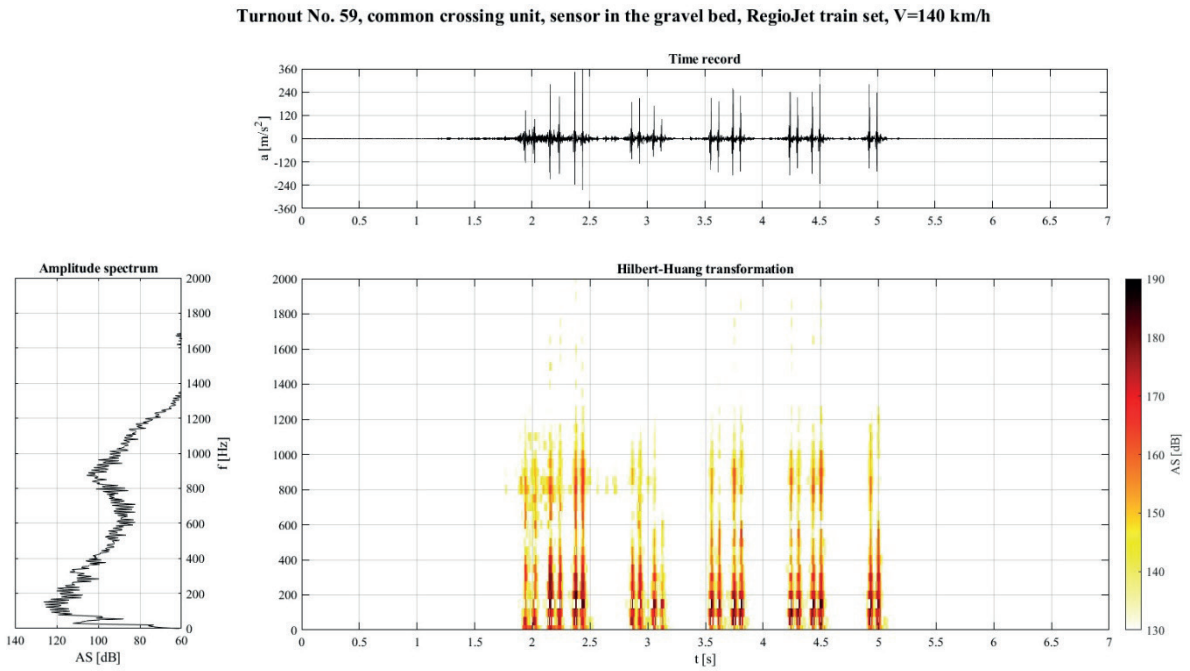

Figure 4 *Time, frequency and time-frequency characteristics of the vibrations, sensor in the gravel bed, turnout no. 59 - common crossing unit, vertically direction, RegioJet, speed 140 km·h^{-1}*

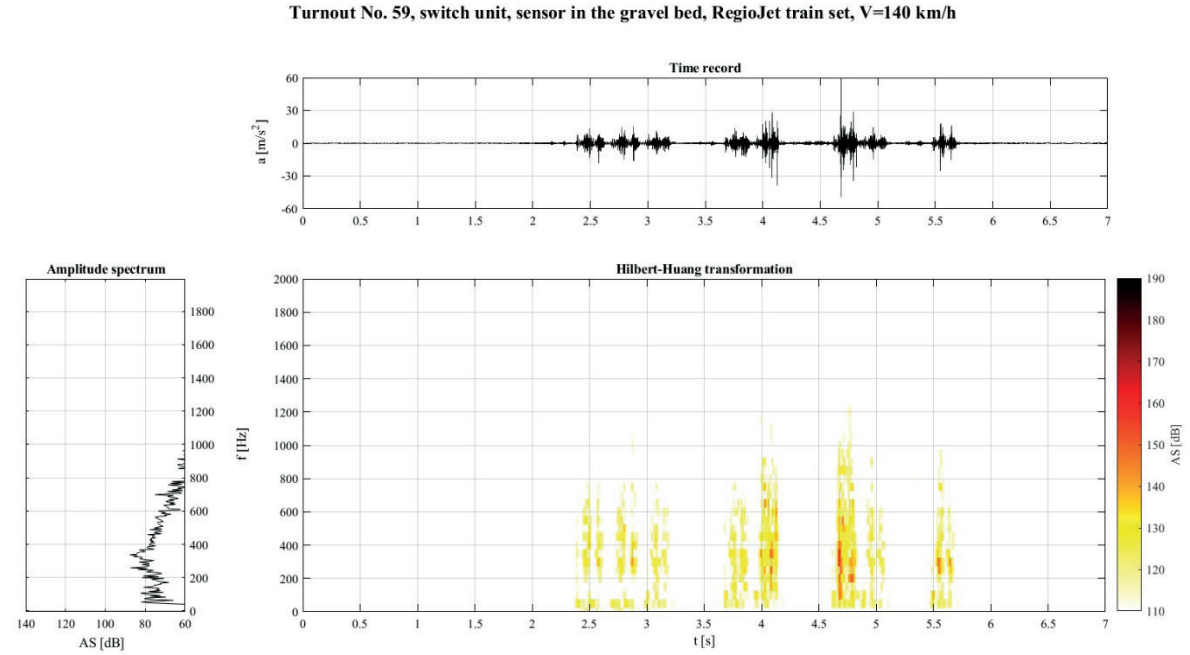

Figure 5 *Time, frequency and time-frequency characteristics of the vibrations, sensor in the gravel bed, turnout no. 59 - switch unit, vertically direction, RegioJet, speed 140 km·h^{-1}*

were measured when the set wheel passes from the wing rail to the common crossing unit tip (Figure 4) compared to the passage of the train set through the switch unit (60 m·s^{-1}) (Figure 5). The time recording of vibrations from the common crossing unit shows the course of the signal composed of a series of very narrow shocks from the wheels of a passing train set. Thus, a relatively large part of the vibrational energy is transferred to the gravel bed.

From the time course found in the switch unit of the turnout, it is clear that the course of acceleration has a different character. The course is much smoother, there are not so outlined individual passages of the wheels of the set.

The frequency spectrum (Figure 4) obtained from the running of the trainset through the common crossing unit shows several frequency clusters with maximum values at the frequencies 30 Hz, 150 Hz, 230 Hz, 320 Hz,

520 Hz, 880 Hz and 1.7 kHz. The highest spectrum value (125 dB) was reached at a frequency of 150 Hz. The frequency spectrum obtained from the running of the trainset through the switch unit (Figure 5) also shows several significant frequency components (80 Hz, 110 Hz, 200 Hz, 260 Hz, 340 Hz and 700 Hz). The highest value of the spectrum (87 dB) was reached at a frequency of 340 Hz.

The same conclusions are drawn with the time-frequency analysis by the Hilbert Huang transform method (middle graphs of Figures 4 and 5). In contrast to the classical frequency analysis performed using the Fourier transform, the time distribution of significant frequency components is also evident from these graphs.

Even in the case of this analysis, it is clear that a higher peak in the time-frequency plane was achieved in the case of passing the wheels of the trainset through the railway common crossing unit. Note that the graphs show a very accurate time localization of individual frequency components.

4 Conclusions

The paper was devoted to the comparison of dynamic effects from the train sets acting on the common crossing and switch unit of the turnout. To compare the selected dynamic parameters excited by the train set, turnout No. 59 was selected. This turnout is located in the Chocen railway station. The paper presents a simplified variant of a certified methodology focused on analysis of the vibrations propagation of turnout structures.

The paper also includes a theoretical analysis and practical application of the Hilbert-Huang transform for evaluation of dynamic phenomena occurring in a turnout. This lesser-known and less used transform belongs to the group of time-frequency procedures particularly suitable for analysis of the nonlinear, transient and non-stationary signals.

The Hilbert-Huang transform represents a certain alternative to, for example, the Fourier transform or the Wavelet transform, or to other time-frequency methods. Note that the Hilbert-Huang transform analyses the signal in a different way, i.e. not by decomposing it into predefined functions such as trigonometric functions, mother wavelet, etc., but into functions defined based on the signal under investigation.

Thanks to the calculation method, it can be used in a wide range of applications. For example, the removal of noise in the measured signal, the visualization of various sources and mechanisms, the analysis of image data etc. It can be reasonably assumed that this transformation will also find significant application in the field of railway engineering, especially in evaluation of the short-term dynamic effects from passing trains. The outputs of the Hilbert-Huang transform can be very well coupled with selected machine classification and identification methods.

According to the performed analysis, it is obvious that in most cases the higher acceleration values were obtained in the common crossing unit of the turnout in the passing railway sets than in the switch unit. Only for the trains pulled by locomotives of the 150 and 151 series the case was opposite. It can be assumed that this fact is influenced by the technical condition of the locomotives of the 150 and 151 series, as well as their different dynamics of passing through the turnout sections in question. This fact has also been observed at other locations during other measurement campaigns. Certainly, this fact is very significantly influenced by different mechanisms of dynamic effects in the heart and change of turnouts, as well, leading to vibrations propagation.

The Hilbert Huang transform generally offers a comprehensive tool for the analysis of transient and non-stationary signals. Based on the experience gained by the authors, its use can also be recommended for the time-frequency analysis of short-term dynamic phenomena occurring in railway structures. This method can be successfully applied not only in the analysis of railway superstructure samples measured in the laboratory, but in the evaluation of real structures, as well.

Based on the analyses performed, it can be concluded that the methodology used provides good results and conclusions. The measured and calculated quantities are characterized by sufficient accuracy and interpretability. The time and frequency analysis tools of the signals have also contributed very well to the quality of the measured data.

The authors recommend continuing the work performed, focusing on turnouts of various types and geometric parameters and focusing on both the common crossing and the switch unit of the turnout. Further analysis and development of the research methods will contribute to a better understanding of the dynamic stress of turnouts from passing trainsets, which will lead to development of the new structures with longer service life and with lower maintenance costs.

Acknowledgements

This paper was supported by the project FAST-S-21-7401, “Evaluation of dynamic effects acting on a structure by advanced mathematical analysis methods”.

References

[1] MORAVCIK, M. Analysis of vehicle bogie effects on track structure - nonstationary analysis of dynamic response. *Communications - Scientific Letters of the University of Zilina* [online]. 2011, **13**(3), p. 33-40. ISSN 1335-4205, eISSN 2585-7878. Available from: http://komunikacie.uniza.sk/index.php/communications/article/view/860

[2] KAEWUNRUEN, S., REMENNIKOV, A. M. Field trials for dynamic characteristics of railway track and its components using impact excitation technique. *NDT & E International* [online]. 2007, **40**(7), p. 510-519. ISSN 0963-8695. Available from: https://doi.org/10.1016/j.ndteint.2007.03.004

[3] KASSA, E., ANDERSON, C., NIELSEN, J. Simulation of dynamic interaction between train and railway turnout. *Vehicle System Dynamics* [online]. 2006, **44**(3), p. 247-258. ISSN 0042-3114, eISSN 1744-5159. Available from: https://doi.org/10.1080/00423110500233487

[4] KAEWUNRUEN, S. Monitoring structural deterioration of railway turnout systems via dynamic wheel/rail interaction. *Case Studies in Nondestructive Testing and Evaluation* [online]. 2014, **1**, p. 19-24. ISSN 2214-6571. Available from: https://doi.org/10.1016/j.csndt.2014.03.004

[5] KOLLMENT, W., O'LEARY, P., HARKER, M., OSSBERGER, U., ECK, S. Towards condition monitoring of railway points: instrumentation, measurement and signal processing. In: 2016 IEEE International Instrumentation and Measurement Technology Conference: proceedings [online]. IEEE. 2016. p. 612-617. Available from: https://doi.org/10.1109/I2MTC.2016.7520434

[6] SMUTNY, J., PAZDERA, L., VUKUSIC, I. Dynamic effects on turnouts evaluation. The certified methodology. Ministry of Transportat of Czech Republic. 124/2014-710-VV/1, 2014.

[7] CHAMPENEY, D. C. *A handbook of Fourier theorems*. New York: Cambridge University Press, 1987. ISBN 9780521265034.

[8] SMUTNY, J. Measurement and analysis of dynamic and acoustic parameters of rail fastening. *NDT & E International* [online]. 2004, **37**(8), p. 119-129. ISSN 0963-8695. Available from: https://doi.org/10.1016/j.ndteint.2003.08.003

[9] HUANG, N. E., SHEN, Z., LONG, S. R., WU, M. C., SHIH, H. H., ZHENG, Q., YEN, N. C., TUNG, C. C., LIU, H.-H. The empirical mode decomposition and the Hilbert spectrum for nonlinear and non-stationary time series analysis. *Proceedings of the Royal Society A* [online]. 1998, **454**(1971), p. 903-995. ISSN 1364-5021, eISSN 1471-2946. Available from: https://doi.org/10.1098/rspa.1998.0193

[10] HUANG, N. E. New method for nonlinear and nonstationary time series analysis: empirical mode decomposition and Hilbert spectral analysis. In: Wavelet Application VII SPIE 4056: proceedings [online]. 2000. p. 197-210. Available from: https://doi.org/10.1117/12.381681

[11] HUANG, N. E., SHEN, S. S. P. *Hilbert-Huang transform and its applications* [online]. World Scientific Publishing, 2005. ISBN 978-981-256-376-7, eISBN 978-981-4480-06-02, p. 1-24. Available from: https://doi.org/10.1142/5862

[12] HUANG, N. E., WU, Z. A review on Hilbert-Huang transform method and its applications to geophysical studies. *Reviews of Geophysics* [online]. 2008, **46**(2), p. 1-23. eISSN 1944-9208. Available from: https://doi.org/10.1029/2007RG000228

[13] HUANG, N. E., CHEN, X., LO, M.-T., WU, Z. On Hilbert spectral representation: a true time-frequency representation for nonlinear and nonstationary data. *Advances in Adaptive Data Analysis* [online]. 2011, **3**(01n02), p. 63-93. ISSN 1793-5369, eISSN 1793-7175. Available from: https://doi.org/10.1142/S1793536911000659

[14] TORRES, M. E., COLOMINAS, M. A., SCHLOTTHAUER, G. S., FLANDRIN, P. A complete ensemble empirical mode decomposition with adaptive noise. In: IEEE International Conference on Acoustic, Speech and Signal Processing ICASSP 2011: proceedings [online]. IEEE. 2011. p. 4144-4147. Available from: https://doi.org/10.1109/ICASSP.2011.5947265

[15] JUNSHENG, C., DEJIE, Y., YU, Y. Research on the intrinsic mode function (IMF) criterion in EMD method. *Mechanical System and Signal Processing* [online]. 2004, **20**(4), p. 817-824. ISSN 0888-3270. Available from: https://doi.org/10.1016/j.ymssp.2005.09.011

[16] ZHANG, R. R., MA, S., SAFAK, E., HARTZELL, S. Hilbert-Huang transform analysis of dynamic and earthquake motion recordings. *Journal of Engineering Mechanics* [online]. 2003, **129**(8), p. 861-875. ISSN 0733-9399, eISSN 1943-7889. Available from: https://doi.org/10.1061/(ASCE)0733-9399(2003)129:8(861)

[17] CHIANG, W. L., CHIOU, D. J., CHEN, C. W., TANG, J. P., HSU, W. K., LIU, T. Y. Detecting the sensitivity of structural damage based on the Hilbert-Huang transform approach. *Engineering Computations* [online]. 2010, **27**(7), p. 799-818. ISSN 0264-4401. Available from: https://doi.org/10.1108/02644401011073665

[18] RILLING, G., FLANDRIN, P., GONCALVES, P. On empirical mode decomposition and its algorithms. In: IEEE-EURASIP Workshop on Nonlinear Signal and Image Processing NSIP2003: proceedings. IEEE. 2003.

[19] PUTRA, T., ABDULLAH, S., NUAWI, M. Z., YUNOH, M. F. M. The Morlet and Daubechies wavelet transforms for fatigue strain signal analysis. *Applied Mechanics and Materials* [online]. 2018, **471**, p. 197-202. ISSN 1662-7482. Available from: https://doi.org/10.4028/www.scientific.net/AMM.471.197

[20] JANOSTIK, D., NOHAL, V., SEELMANN, H., SMUTNY, J. The continuous monitoring of selected railway structures using the autonomous data logger. *Communications - Scientific Letters of the University of Zilina* [online]. 2020, **22**(2), p. 88-96. ISSN 1335-4205, eISSN 2585-7878. Available from: https://doi.org/10.26552/com.C.2020.2.88-96